Computed Tomography Based Attenuation Correction in PET/CT: Principles, Instrumentation, Protocols, Artifacts and Future Trends

Mohammad Reza Ay, PhD[1,2,3] and Saeed Sarkar, PhD[1,2]

[1] Department of Medical Physics and Biomedical Engineering, School of Medicine, [2] Research Center for Science and Technology in Medicine, Medical Sciences/University of Tehran, Tehran, Iran, [3] Division of Nuclear Medicine, Geneva University Hospital, Geneva, Switzerland

ABSTRACT

The advent of dual-modality PET/CT imaging has revolutionized the practice of clinical oncology, cardiology and neurology by improving lesions localization and the possibility of accurate quantitative analysis. In addition, the use of CT images for CT-based attenuation correction (CTAC) allows to decrease the overall scanning time and to create a noise-free attenuation map (μmap). The near simultaneous data acquisition in a fixed combination of a PET and a CT scanner in a hybrid PET/CT imaging system with a common patent table minimizes spatial and temporal mismatches between the modalities by elimination the need to move the patient in between exams. As PET/CT technology becomes more widely available, studies are beginning to appear in the literature that document the use of PET/CT in a variety of different cancers, including lung, thyroid, ovarian, lymphoma, and unknown primary cancers, and for general oncology, cardiology and neurology applications. Specific applications of PET/CT, such as those for radiation therapy planning, are also being explored. The purpose of this review paper is to introduce the principles of PET/CT imaging systems and describe the sources of error and artifact in CT-based attenuation correction algorithm. This paper also focuses on recent developments and future trends in hybrid imaging and their areas of application. It should be noted that due to limited space, the references contained herein are for illustrative purposes and are not inclusive; no implication that those chosen are better than others not mentioned is intended.

Key Words: PET/CT, X-ray CT, Attenuation correction, CTAC, Hybrid imaging, Contrast medium, Artifact.

Corresponding Author: Dr Mohammad Reza Ay, Department of Medical Physics and Biomedical Engineering, School of Medicine, Tehran University of Medical Sciences, Enghelab Ave. Tehran, Iran.
E-mail: mohammadreza_ay@sina.tums.ac.ir

1. Introduction

Diagnostic imaging began in the first decade of the 20th century after discovery of x-rays by Professor Roentgen. The development of radiology as a first imaging technique grew at a good pace until World War II. Extensive use of x-ray imaging during the second World War, and the advent of the digital computer and new imaging modalities like ultrasound, magnetic resonance imaging and nuclear medicine have combined to create an explosion of diagnostic imaging techniques in the past three decades [1].

Clinical diagnosis is often supported by several imaging modalities which provide complementary information. Generally, this information can be classified as anatomical and functional. Diagnosis, staging and re-staging of cancer, as well as the monitoring and planning of cancer treatment, has traditionally relied on anatomic imaging like CT and MRI. One of the disadvantages of anatomical imaging techniques is their inability to characterize the tumor. Lesions need to be characterized whether they are benign or malignant and if malignant it would be helpful to know whether proliferation is slow or fast. Necrotic, scar and inflammatory tissue often cannot be differentiated from malignancy based on anatomic imaging alone. Anatomical imaging has high sensitivity for detection of structural changes, but a low specificity further characterization of these abnormalities. SPECT and PET are imaging techniques that provide information on physiology rather than anatomy. These modalities have been used for evaluation of tumor metabolism, difference between tumor recurrence and radiation necrosis, detection of hypoxic areas of the tumor, and other functional imaging [2].

There are many instances in which it would be desirable to integrate the information obtained from two modalities of the same patient. The poor anatomical resolution of PET and SPECT images can be improved by integration with high resolution images delivered by CT or MRI. The resulting image could be named as hybrid image. Figure 1 shows a transaxial slice from human chest acquired with different modalities, left (CT, anatomical information), middle (PET, functional information) and right (PET/CT, fusion of anatomical and functional information).
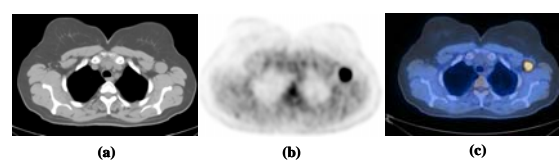

Figure 1: Transaxial slice from chest acquired with different modalities: **(a)** CT; **(b)** PET; and **(c)** hybrid PET/CT.

Historically, the first dual-modality device was a combination of SPECT and CT. The pioneering work by Hasegawa et al.[3] and Lang et al. [4] combined anatomical and functional images by using a single detector for both modalities. In addition, the x-ray CT images were used to provide an attenuation map for attenuation correction of SPECT data [5]. The first commercial SPECT/CT produced by GE Healthcare (Milwaukee, WI) was introduced in 1999 [6].

Although the idea of combining PET and CT was proposed in 1994, the first prototype dedicated PET/CT scanner was installed in the University of Pittsburgh Medical Center in 1998 [7]. The prototype was developed in collaboration with CTI PET systems (Knoxville, TN) and the first commercial

system approved by FDA was presented at the 2000 Society of Nuclear Medicine meeting in St. Louis. Thereafter, GE Healthcare (Milwaukee, WI) introduced a PET/CT system, now named Discovery LS, at the 2000 Radiological Society of North America (RSNA) meeting in Chicago and Philips Medical Systems (Milville, TN) presented their version of combined PET/CT, the Gemini, at the RSNA meeting in 2001. Combined PET/CT scanners have been in production for less than 7 years and the technology is undergoing rapid evolution. The introduction of new geometrical designs, scintillator crystals and fast electronics in PET components and in parallel increasing the number of detector rows and reduction of rotation time in CT scanners will potentially increase the performance of PET/CT scanners [8].

The advent of PET/CT scanners is considered as a major advance in medical imaging technology and health care. PET/CT systems offer significant advantages over stand alone PET including decreased overall scanning time and increased accuracy in lesions localization. As the name implies, PET/CT combines the information produced by two sophisticated imaging modalities: the functional information from PET with the anatomical information from CT into a single procedure [9]. The combination of two complementary modalities significantly increases the diagnostic accuracy compared to each of the two modalities, as well as the two imaging modalities viewed side-by-side [10-14], in addition PET/CT improves disease localization and facilitates treatment planning for radiation oncology or surgery [6]. The number of inconclusive PET findings will be reduced by accurate identification of the site of the activity

accumulation. This finding may be due to pathologically increased (tumor) turnover, pathologically increased turnover in a nonmalignant process (e.g., inflammation, thyroid nodule), or increased but physiological uptake in an activated organ (e.g., fatty tissue, muscle, endocrine gland). The high-resolution anatomical information from PET/CT improves the differentiation of physiological (normal) uptake of ^{18}F-fluorodeoxyglucose (FDG) and other radiopharmaceuticals from that associated with disease, and thereby can reduce false positive errors in comparison to lesion characterization when PET imaging is used alone [15].

2. PET/CT Physics and Instrumentation

In current PET/CT designs, the two scanners (PET and CT) are physically separate with the CT position anterior of the PET, in the same cover (Fig. 2). The advantage of this minimal hardware integration is that each system can use the latest technology, independently. In the last seven years, since the introduction of PET/CT in clinical area, there have been significant advances in both CT and PET technology and consequently these advances become incorporated into current generation PET/CT scanners [9].
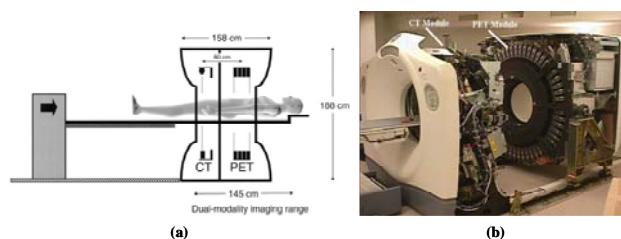

Figure 2: (a) Schematic illustration of a PET/CT scanner. Reprinted with permission from ref. [8] **(b)** Individual PET and CT modules placed in one cover in a commercial Discovery LS PET/CT scanner. Courtesy of GE Healthcare.

X-ray computed tomography is an imaging modality that produces cross-sectional images representing the x-ray attenuation properties of the body. Unlike conventional tomography, CT does not suffer from interference from structures in the patient outside the slice being imaged. This is achieved by irradiating only thin slices of the patient.

Compared to planar radiography, CT images have superior contrast resolution, i.e, they are capable of distinguishing very small differences between tissues attenuation. Two steps are necessary to derive a CT image: firstly, physical measurements of the attenuation of x-rays traversing the patient in different directions; and secondly mathematical calculations of the linear attenuation coefficients, μ, all over the slice. The patient remains on the examination table while the x-ray tube rotates in a circular or spiral orbit around the patient in a plane perpendicular to the length-axis of the patient. The data acquisition system is an array of several hundred small separate detectors placed on the opposite side of the patient [16].

PET imaging relies on the nature of positron decay. When a nucleus undergoes positron decay, the result is a new nuclide with one fewer proton and one more neutron, as well as the emission of positron and a neutrino. As positrons pass through matter, they experience the same interactions as electrons, including loss of energy through ionization and excitation of nearby atoms and molecules. After losing enough energy and travelling a given distance in matter (depending the initial energy of the positron), the positron will annihilate with a nearby electron and two photons in opposite directions are emitted each with energy of 511 keV. These photons are the basis of coincidence detection and coincidence imaging. PET imaging systems detect annihilation events by means of several rings of photon detectors that surround the patient. When two matching photons originating from the same annihilation event are recorded within nanoseconds of each other, two opposite detectors register a coincidence event along the line between both detectors. The PET system then registers all lines of response between each detector pair registering a coincidence event during the scan. At the end of the acquisition, there will be areas of overlapping lines which indicate more highly concentrated areas of radioactivity, according to the tracer distribution within the patient body. Then the raw data can be reconstructed to create cross sectional images representing the radioactivity distribution into the tissues [17].

3. Attenuation Correction Strategies in PET

Several physical factors can degrade image quality and quantitative accuracy in PET. These factors include but are not limited to: scattered photons [18], physiological as well as patient motion [19], attenuation of photons [20], partial volume effect [21], parallax effect [22], positron range and non-collinearity [23]. The most important factor is attenuation of photons in tissues, which can affect both visual interpretation and quantitative accuracy of PET data [20]. Attenuation correction has been shown to improve image quality, lesion detection, staging and management of patients in clinical oncology compared to non-attenuation corrected images [24].

Reliable attenuation correction methods for PET require determination of an attenuation map, which represents the spatial distribution of linear attenuation

coefficients at 511 keV for the region under study. After the attenuation map is generated, it can be incorporated into image reconstruction algorithms to correct the emission data for errors contributed by photon attenuation (Fig. 3). The methods for generating the attenuation maps can be categorized in two main classes: transmissionless methods and transmission-based methods [20].
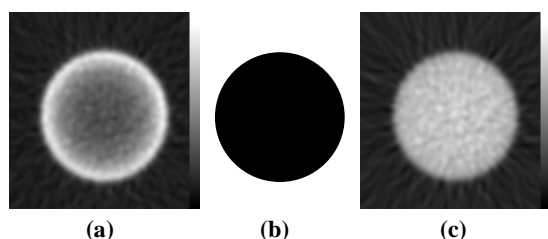

(a)   **(b)**   **(c)**

Figure 3. Illustration of reconstruction artifact resulting from lack of attenuation correction for uniform distribution of activity in a cylindrical phantom. **(a)** Reconstructed image without attenuation correction. **(b)** Uniform attenuation map at 511 keV. **(c)** Same slice as **(a)** after applying attenuation correction. Reprinted with permission from ref. [20].

Transmissionless correction methods are based on calculation of boundary and distribution of attenuation coefficients by means of approximate mathematical methods, statistical modeling for simultaneous estimation of attenuation and emission distribution and consistency conditions criteria. It is generally difficult to generate accurate attenuation map using transmissionless methods especially in whole-body imaging with more complex juxtapositions of media with different attenuation properties and irregular contours. Therefore, transmissionless techniques have limited value for clinical applications [20].

In clinical applications, in which the attenuation coefficient distribution is not known *a priori*, and for areas of inhomogeneous attenuation such as the chest,

more adequate methods (transmission-based methods) must be performed to generate the attenuation map. This includes transmission scanning using external radionuclide sources, x-ray CT scanning and segmented MRI data. In stand alone PET systems, the most widely used attenuation correction technique is radionuclide transmission scanning before (pre-injection), during (simultaneous) or after (post-injection) emission scan [25]. The use of x-ray CT scans offers the advantage of higher photon fluence rates and faster transmission scan, in addition to true anatomic imaging and localization capability that can not be obtained using radionuclide transmission scans [20]. The clinical use of MRI-based attenuation correction techniques currently is limited to brain imaging. In this method the T1-weighted MR images are realigned to preliminary reconstructed PET data using an automatic algorithm and then segmented to classify the tissues in different categories depending on their density and composition. Then the theoretical tissue-dependent attenuation coefficients are assigned to the related voxels in order to generate an appropriate attenuation map [26].

4. CT-Based Attenuation Correction in PET

Attenuation maps generated for attenuation correction have traditionally been obtained using external radionuclide sources. This process is identical conceptually to the process of generating CT images with an x-ray tube that transmits radiation through the body, with transmitted intensity recorded by an array of detector elements. The transmission data can then be reconstructed using a tomographic algorithm that inherently calculates the attenuation coefficients at each point in the reconstructed slice.

The reconstructed CT image contains pixel values that are related to the linear attenuation coefficient at that point in the patient, calculated from the effective CT energy at operational tube voltage of scanner. However, the attenuation map at 511 keV can be generated from the CT images to correct the PET emission data for photon attenuation [20, 27]. CT-based attenuation correction offers four significant advantages [28]: first, the CT data will have much lower statistical noise; second, the CT scan can be acquired much more quickly than a radionuclide transmission scan; third is ability to collect uncontaminated post-injection transmission scan and forth, using the x-ray transmission scan eliminates the need for PET transmission hardware and periodic replacement of ^{68}Ge/^{68}Ga positron sources. A potential benefit not yet fully explored is the direct incorporation of anatomical information derived from the CT data into the PET image reconstruction process and correction for partial volume effect [29].

As noted above, CT inherently provides a patient-specific measurement of the linear attenuation coefficient at each point in the image. However, the linear attenuation coefficient measured with CT is calculated at the x-ray energy rather than at the 511 keV. It is therefore necessary to convert the linear attenuation coefficients obtained from the CT scan to those corresponding to the 511 keV (Fig. 4). Several conversion strategies have been developed including scaling [30], segmentation [28], hybrid (segmentation/scaling) [31], piece-wise linear scaling [32], and dual-energy decomposition methods [33]. In the following, a short description of the nominated methods is presented.

Scaling. The scaling approach estimates the attenuation image at 511 keV by multiplying the CT image by the ratio of attenuation coefficients of water at CT and PET energies. A single effective energy is chosen to represent the CT spectrum, typically in the range of 50-80 keV [30].

Segmentation. This method forms the attenuation image at 511 keV by segmenting the reconstructed CT image into different tissue types. The CT image value for each tissue type is then replaced with appropriate attenuation coefficients at 511 keV. Typical choices for tissue types are soft tissue, bone, and lung [28, 35].

Hybrid. This method appears to be the most promising and is based on a combination of the scaling and segmentation methods above using the fact that for most materials except bone, the ratio of the linear attenuation coefficient at any two photon energies is essentially constant [31].

Piece-wise linear. In this method, series of CT scans from a known material (e.g. K_2HPO_4 solution) with different concentrations is performed. A calibration curve is then generated in which the measured CT number is plotted against the known attenuation coefficients at 511 keV. The resulting calibration curve is piece-wise linear and covers the range of linear attenuation coefficients commonly encountered in the body. It should be noted that most commercially available PET/CT scanners use the bi-linear calibration curve method [32].

Dual-energy decomposition. A technically challenging approach is to acquire the CT image at two different photon energies (e.g. 40 keV and 80 keV) and use these data to extract the individual photoelectric and Compton contributions to linear attenuation coefficients. The different contributions can then be scaled separately in energy [33].
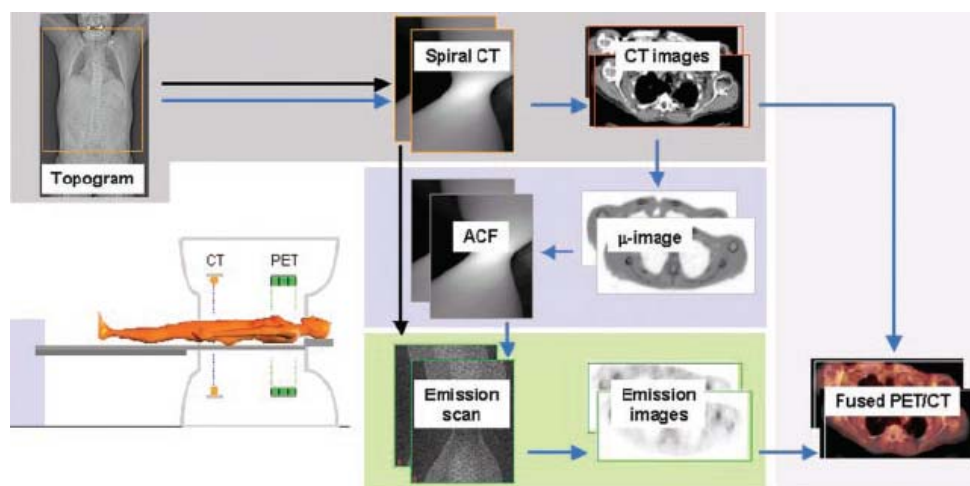
Figure 4. Principle of CT-based attenuation correction method on commercial PET/CT scanners.
Reprinted with permission from ref. [34].

In addition to the energy conversion, there are other issues that must be considered in using CT to generate attenuation maps for correction of emission data. CT fundamentally has a higher spatial resolution and is reconstructed in a finer image matrix than PET. Typically, 512×512 CT images can be down-sampled to the same image format (e.g. 64×64, 128×128, 256×256) as that used for reconstruction of PET emission data. CT images also must be smoothed with a Gaussian filter using an appropriate kernel to match the spatial resolution of emission data (Fig. 5) [20].

5. Sources of Error and Artifact in CTAC

PET/CT systems offer significant advantages over stand alone PET including decreased overall scanning time and increased accuracy in tumor localization and detectability [6]. However, the use of CT images for attenuation correction of PET data is known to generate visible artifacts in the resulting PET images in some cases [20]. Commercial, CT reconstruction algorithms cannot account for the presence of metal

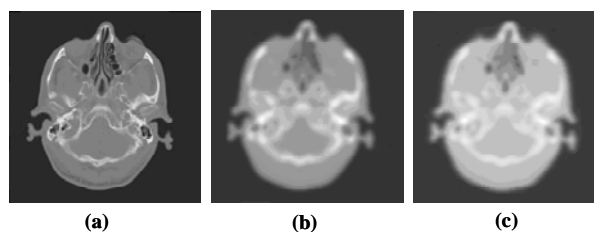implants, such as dental fillings or prostheses properly.

Figure 5. (a) Original CT image acquired at 120 kVp with matrix size 512×512; **(b)** the slice in **(a)** after down-sampling to 128×128 and Gaussian smoothing with FHHM=6 mm. **(c)** Attenuation map of the slice in (b) at 511 keV converted using a bi-linear calibration curve.

This results in steak artifacts, which are propagated into PET images by the attenuation correction process [36-40]. The transformation of attenuation coefficients at x-ray energies to those at 511 keV works well for soft tissues, bone, and air, but not for dense CT contrast agents such as iodine or barium [2, 41-48].
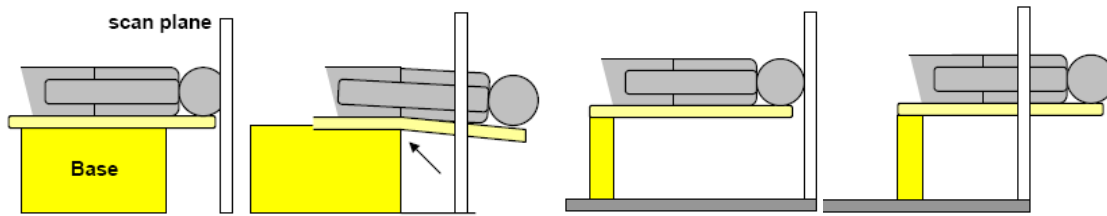
Figure 6. (a) A normal CT patient couch, the arrow shows couch flex **(b)** A new designed CT couch for PET/CT in order to remove couch flex. Reprint with permission from ref. [63].

Mismatches due to uncoordinated respiration as well as patient movement result in incorrect attenuation-corrected PET images [49-55]. Truncation artifacts due to limited CT field-of-view are frequently observed in PET/CT imaging of large patients [34]. These artifacts, however, can be minimized or avoided by careful acquisition protocols or appropriate correction schemes [56]. The x-ray tube settings (kVp and mA) are another important issue that should be considered during CT examination in order to have a noise free attenuation map [57, 58] and decrease patient dose [59-61]. In the following, an overview of different sources of error and artifact in CT-based attenuation correction in PET/CT systems is presented.

5.1. Misalignment between PET and CT Images

The advent of hybrid PET/CT systems has simplified image registration since the PET and CT data sets are collected sequentially on the same system without the need for the patient to move to another scanner. This removes the image registration problem induced by different patient set-up positions [62]. Once the CT scan is complete, the patient couch is moved further into the gantry to commence the PET scan. The two data sets can be considered to be inherently registered; just the distance between the PET and CT

positions needs to be taken into account. Generally, there are two registration issues that must be considered; first the misalignment of CT and PET modules during the installation of the PET/CT scanner owing to the fact that current PET/CT systems consists of individual PET and CT systems adjacent to one another. Second, is the flex of patient couch. As the couch is moved into the gantry toward the PET module after CT scanning, more of the patient's weight is taken by part of the couch that is unsupported by the base. For accurate image registration it is important that the degree of couch flex does not change as the patient is moved from CT to PET acquisition position. This would cause registration problems in PET/CT. More recently with the advent of pedestal/couch design configurations the degree of flex keeps constant regardless of how far the couch is moved into the gantry (Fig. 6). This ensures that the vertical position of the patient is the same for the CT and PET acquisitions [63].

5.2. Patient and Respiratory Motion

Mismatches between CT and PET images due to the physiological motion (respiratory motion) as well as patient movement have been described as a source of potential artifacts of PET emission images obtained using CT-based attenuation correction [19]. Most of

patient movement and positioning errors in PET/CT examinations may be overcome using immobilization tools [12, 56].
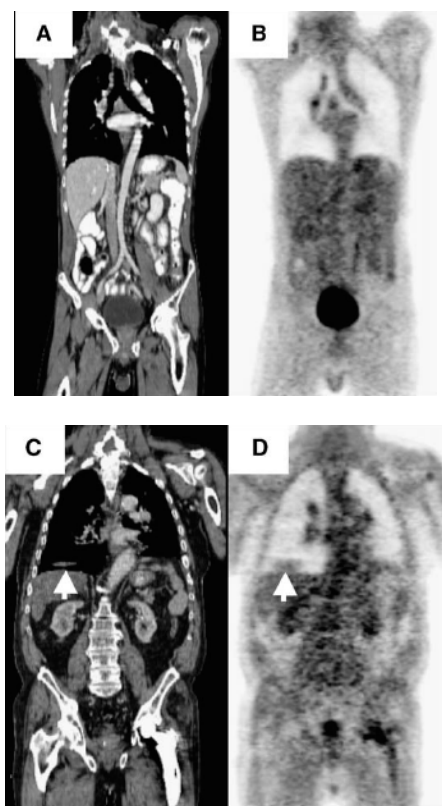

Figure 7. Effect of respiratory motion in CT propagates into the emission image through the attenuation correction. **(a)** CT image using breathhold during thorax scan. **(b)** PET image using attenuation correction factors from Fig. 7a. **(c)** CT image of different patient during normal breathing. **(d)** PET image using attenuation correction factors from Fig. 7c clearly shows an artifact above liver (arrow) caused by the liver dome being mirrored at the right lung base. Reprint with permission from ref. [76].

Respiratory artifacts are particularly severe when standard breath-hold techniques with maximum inspiration are transferred directly from clinical CT standalone protocols to combined PET/CT without further adaptation. These artifacts are caused by the mismatches of anatomy of thoracic and abdominal organs at maximum inspiration in CT images versus the anatomy when averaging over many respiratory cycles during the PET study [34]. Qi *et al.* [64]

studied how the errors from respiratory mismatch propagate into the PET image through the CT-based attenuation correction. Goerres *et al.* [65] have compared the accuracy of PET/CT image alignment in the thorax and abdomen. They reported normal expiration and free breathing to provide the best match in the thorax area in 53% and 23% of patients, respectively. The PET and CT alignment in the abdominal area was satisfactory in both protocols [66]. However, if the respiratory commands are not adequately followed by the patient, the reconstruction of emission data without attenuation correction is suggested [56]. To account for the internal organ motion due to respiration, nowadays, 4D-PET/CT protocol has been developed. Such protocol enables the PET and CT data to be individually divided into different phases of the respiratory cycle thus permitting data from both modalities to be matched at the same phase. However, the success of such a method does not depend on the technology alone, but primarily on the cooperation of the patient, and his/her ability to maintain a regular breathing pattern [67-73]. In the absence of necessary hardware for respiratory gating, several groups have attempted to minimize the respiratory artifacts using available hardware [74] or modifying the acquisition protocols [72]. Beyer *et al.* [49] shown in whole-body PET/CT imaging of normally breathing patients, respiration-induced artifacts are reduced in both magnitude and prominence for PET/CT systems employing CT components of six or more detector rows. Pan *et al.* [75] have proposed using respiratory-averaged CT images in order to minimize the respiratory induced artifact in CTAC. Figure 7 shows the effects of respiratory motion in an image. The CT in Fig. 7a, taken during a breath hold at normal expiration, has no errors and consequently the attenuation-corrected

PET image (Fig. 7b) has no errors. Figure 7c presents a CT taken during normal breathing with a liver artifact and Fig. 7d shows how this error appears in the attenuation-corrected PET image.

5.3. Truncation

During CT imaging of obese patients and patients with their arms down, part of the anatomy may extend beyond the boundaries of the CT field of view (50 cm) and is not reconstructed in CT. This truncation artifact will propagate errors to the CT-based attenuation correction which is based on fully reconstructed CT images including all anatomies which appears in PET images. In the presence of truncation errors in CT images, the reconstructed emission images appear to be masked by the truncated CT. The tracer distribution is then only partially recovered outside the CT field of view as some bias of the reconstructed activity distribution inside the field of view is observed (Fig. 8) [77-79]. There are two approaches for truncation artifact correction. In the software approach, several algorithms have been suggested to extend the truncated CT projections to recover truncated parts of the attenuation map [80]. In the hardware approach, most manufacturers offer PET/CT scanners with a patient port of 70 cm for both PET and CT modules to avoid truncation of CT images for most of the patients even with arms in down position [8].

5.4. Beam Hardening and X-ray Scattered Radiation

The polyenergetic x-ray spectra used during CT imaging makes it subject to beam hardening artifact cased by the absorption of low energy x-rays as they pass through the patient's body. The direct consequence is that the linear attenuation coefficient

calculated for thick body regions is lower than thin regions. This effect generates cupping and streak artifact in the reconstructed CT image and makes it not acceptable for diagnostic purposes. Furthermore, the resulting erroneous CT-based attenuation correction subsequently propagates the error to the calculated activity concentration in PET images [56]. Although beam hardening effect correction algorithms [81] implemented as part of CT reconstruction software, this effect is still visible when having the patient's arms in the field-of-view or for obese patients during CT scanning using standard whole-body PET/CT protocols [56].
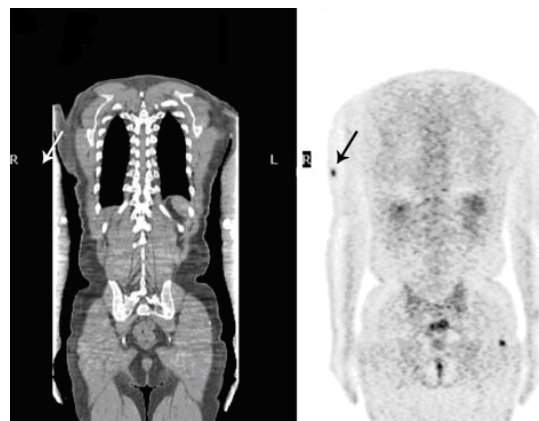

Figure 8. 54-y-old man with history of metastatic melanoma (arrow). CT image appears truncated (left) and biases PET attenuation-corrected image (right). Reprint with permission from ref. [79].

The contamination of CT data with scattered radiation reduces reconstructed CT numbers and introduces cupping artifacts in the reconstructed images. This effect is more pronounced in next generation of CT scanners with large area flat-panel detector that seems to be candidates as CT module in next generation of PET/CT scanners with panel-based PET module [8].
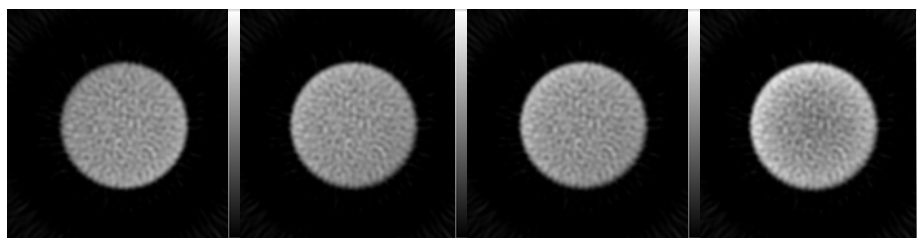
Figure 9. Reconstructed images of Monte Carlo simulated emission data corrected for attenuation using from left to right: CAC, CTAC primary, CTAC total fan-beam and CTAC total cone-beam. Reprint with permission from ref. [43].

Ay and Zaidi [43, 82] quantified the contribution of x-ray scatter during the CTAC procedure for commercially available multi-slice CT and prototype large area flat panel detector-based cone-beam CT scanners using Monte Carlo simulation. They reported the magnitude of scatter in CT images for the cone-beam geometry is significant and might create cupping artifacts in reconstructed PET images during CTAC; however, its effect is small for current generation multi-slice fan-beam CT scanners using septa between detector elements, but should preferably be corrected during CT reconstruction to avoid quantification bias. Their results substantiate the important role of antiscatter collimation and robust scatter correction algorithms which certainly will be implemented in future generation flat panel based PET/CT scanners when used for quantitative measurements. Figure 9 shows the reconstructed images of a uniform distributed activity in a cylindrical water phantom after attenuation correction of simulated emission data using the ACF sinograms calculated with different methods including calculated AC (CAC) based on the theoretical value of the linear attenuation coefficient of 511 keV photons in water and the generated μmaps using CTAC with the simulated CT image including primary (ideal case), total fan-beam (current multi

slice CT) and total cone-beam (panel base CT) , respectively. The underestimation of ACFs will induce underestimation of activity concentration in the central area of PET images [43].

5.5. Contrast Medium

Although diagnostic quality CT relies on the administration of oral or intravenous contrast agents to allow improved lesion delineation, the presence of positive contrast agents in dual-modality PET/CT systems significantly overestimates the attenuation map in some cases and may generate artifacts during CTAC [41, 45-47]. This is due to the high attenuation coefficient of these materials at the low effective energy of the corresponding x-ray spectra which results in high CT numbers in the region of contrast agent accumulation through misclassification with high density cortical bone [48]. Currently available algorithms for conversion from CT numbers to linear attenuation coefficients at 511 keV are based on the assumption that image contrast in the CT data is contributed by mixtures of air, soft tissue, and bone [32]. The presence of contrast medium complicates this process since two regions that have the same image contrast may indeed have different compositions, for example contributed by bone and soft tissue in one case and iodine/barium contrast and

soft-tissue in another situation [83]. These artifacts are most severe in cases where the contrast media is concentrated, for example in abdominal imaging after the patient swallows a bolus of oral contrast. In this case, the higher densities contributed by the oral contrast media can lead to an overestimation of PET activity [20]. The issue of whether the use of oral contrast medium in dual-modality PET/CT scanning produces medically significant artifacts is still controversial with some studies corroborating [45, 46, 84-87] and others contradicting [43, 44, 47, 48, 88] the fact that the presence of contrast medium can be a source of errors and artifact when the CT data are used for attenuation correction of PET images. However there are different strategies for correction of the contrast agent artifact in CTAC. Some investigators have proposed using separate bi-linear calibration curves for conversion from CT numbers to linear attenuation coefficients at 511 keV for bone-soft tissue and contrast agent-soft tissue combination [28]. Other groups have proposed using image segmentation methods of converting CT numbers to attenuation coefficients that correctly scale contrast enhanced CT images for intravenous and oral agents [89]. Other strategies including the acquisition of both pre-contrast and post-contrast CT scans can be used to minimize possible artifacts contributed by the presence of contrast media [8]. threshold conversion method for whole body imaging and cylindrical threshold correction and global threshold correction method for cardiac imaging are alternative methods [90]. Another well implemented method for correction of oral and intravenous contrast medium artifact in CTAC PET images called segmented contrast correction (SCC) method was proposed by Nehmeh *et al* [48]. This method was evaluated using both phantom and clinical studies and proved to

accurately recover lesion size and uptake. Although several studies have shown that the SCC algorithm is efficient but still limited to simple shapes reflecting the spatial distribution of contrast medium [43, 48]. This limitation makes this efficient algorithm useless in clinical area, where we are facing with irregular shapes of regions containing contrast medium usually found in clinical studies. However, the classification of regions containing bone and contrast agent material in contrast enhanced CT images is a challengious task; due to the fact the CT number of these regions is similar in the majority of clinical cases. More recently an automatic segmentation algorithm has been developed by Bidgoli *et al.* [91] and Ay *et al.* [92] for implementation of SCC algorithm in clinical area. Figure 10 shows image artifact in contrast enhanced PET/CT image and figure 11 shows the accuracy of our newly developed algorithm for automated segmentation and classification of regions containing oral contrast medium in order to correct for artifacts in CT attenuation-corrected PET images using the segmented contrast correction (SCC) algorithm [91, 92].

5.6. Metallic Implant

Some candidate patients for PET/CT imaging have artificial metallic implants, such as artificial joints, metal braces in the spine, chemotherapy ports, hip prosthetic material, dental filling, pacemaker and ICD leads. In standard PET transmission scanning with radionuclides, metal implants causes a little or no artifact while these artifact can be significant in CT energies due to the significantly higher x-ray absorption of high-Z materials (e.g. metals) compared to the low-Z materials (e.g. tissues).
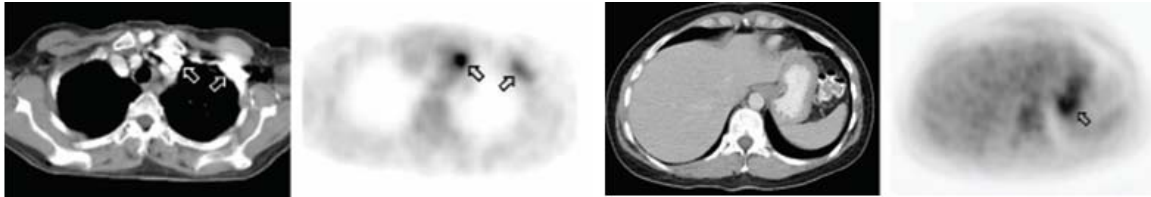
Figure 10. Image artifact in contrast enhanced PET/CT image, **(a)** Bolus passage of intravenous contrast agent in left subclavian and brachiocephalic veins on CT led to areas of apparently increased glucose metabolism on corrected PET **(b)**. Positive oral contrast agent (barium) in stomach on CT image **(c)**. Area of apparently increased glucose metabolism on PET **(d)**. Reprint with permission from ref. [41].
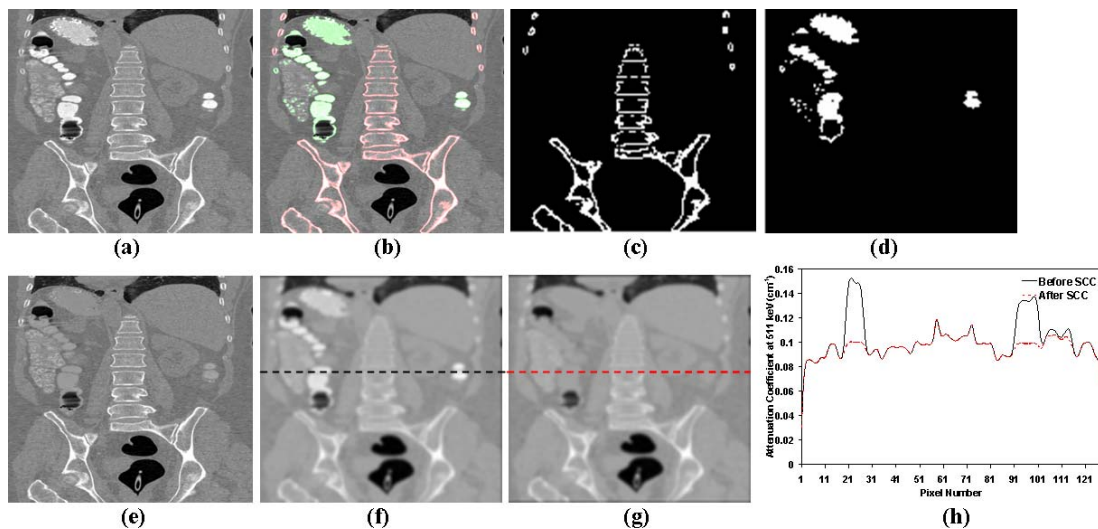

Figure 11. Original contrast enhanced CT image (a), segmented CT image (b), bone objects (c), contrast agent objects (d), original contrast enhanced CT image after applying SCC to the regions segmented as containing contrast agent (e), generated μmap from original CT (f), and generated μmap after SCC (g). Horizontal profiles (position shown in f-g) through generated attenuation maps before and after applying SCC (h).

The presence of streak artifacts caused by metallic implants in CT images may mislead the diagnosis of patients in PET/CT images, particularly when lesions are present in the very vicinity of metallic implants [56]. Several authors addressed the impact of using CTAC on quantitative analysis of PET/CT images in presence of dental metallic implants [40], hip prosthetic material [38], pacemaker and ICD leads [36] and metallic DBS leads used for treatment of Parkinson's disease [43]. Figure 12 shows the overestimation of PET activity in presence of metallic implant.
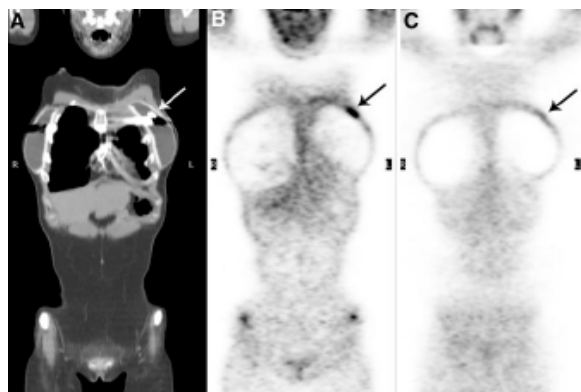
Figure 12. Metal ring on left breast of patient (arrow) produces streaking artifacts and high CT numbers (**a**), resulting in falsely increased radiotracer uptake on PET images with CT attenuation correction (**b**), whereas PET image without attenuation correction shows only background activity at level of metal ring (**c**). Reprint with with persmission from ref. [79].

5.7. Impact of X-ray Tube Voltage

In general, the CT number values in CT images are approximately linearly related to the linear attenuation coefficient of the corresponding tissue type. However, it is well known that the CT images do not precisely correspond to a perfect linear attenuation map at a fixed energy due to the use of polyenergetic x-ray spectra. With the introduction of hybrid PET/CT systems in clinical setting, precise conversion from CT numbers derived from low energy polyenergetic x-ray spectra to linear attenuation coefficients (LACs) at 511 keV became essential in order to apply accurate CT-based attenuation correction to the PET data. Most commercially available PET/CT scanners use the bi-linear calibration curve method, which is generally calculated at a preset tube voltage (120-140 kVp). Since patient CT images may be acquired at different tube voltages depending on patient size and region under study and considering the fact that the CT number of a particular tissue is tube voltage

dependent, it is hypothesized that the use of a single calibration curve calculated at a specific tube voltage for CT images acquired under different scanning conditions might propagate a significant uncertainty during the quantitative analysis of emission data when PET attenuation correction is based on CT [57]. Bai *et al.* [32] argued that the slope of the bi-linear calibration curve for CT numbers higher than 0 HU is tube voltage dependent. Other studies reported on the relevance of deriving tube voltage dependent CTAC schemes for PET/CT [93, 94]. Ay and Zaidi [57] reported both μmaps and ACFs are overestimated when using a calibration curve derived from a tube voltage (140 kVp) higher than the one used during actual CT scanning (120 kVp) of the patient. The behavior is reversed when using the calibration curve derived from a lower tube voltage (80 kVp). In addition they concluded that using a single calibration curve derived under standard scanning conditions during the CTAC procedure to images acquired at different tube voltages does not affect significantly the visual qualitative interpretation and quantitative analysis of PET emission images.
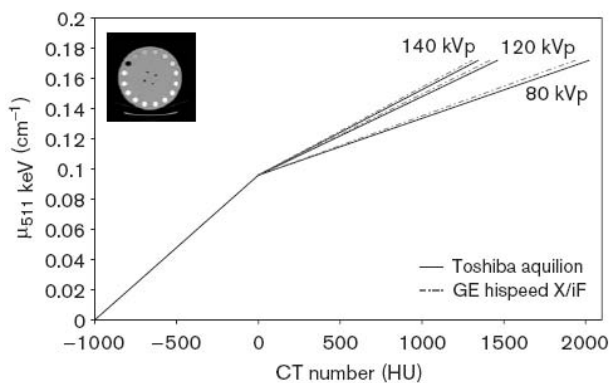

Figure 13. Calculated bi-linear calibration curves for conversion of CT numbers (HU) into linear attenuation coefficients at 511 keV at different tube voltages for both Aquilion and HiSpeed X/iF CT scanners. Reprint with permission from ref. [57].

The same behavior was observed when calibration curves are derived at different tube voltages and used for conversion of CT images acquired at fixed tube voltage [57]. However, a kVp-dependent calibration curve for converting CT Hounsfield units into 511 keV linear attenuation values for attenuation correction in PET/CT studies is highly recommended [57, 93]. Figure 13 shows the calculated bi-linear calibration curves for two commercial CT scanners at different tube voltages (80 kVp, 120 kVp and 140 kVp). The XCOM photon cross sections database [95] was used for calculation of the corresponding linear attenuation coefficients of the inserted solutions at 511 keV.

5.8. Impact of X-ray Tube Current

It is well known that a high tube current improves CT image quality at the expense of increasing patient dose. It was reported that effective doses of 8.81 mSv and 18.97 mSv are delivered to the patient for a whole body CT scan in high-speed and high-quality mode, respectively [60].
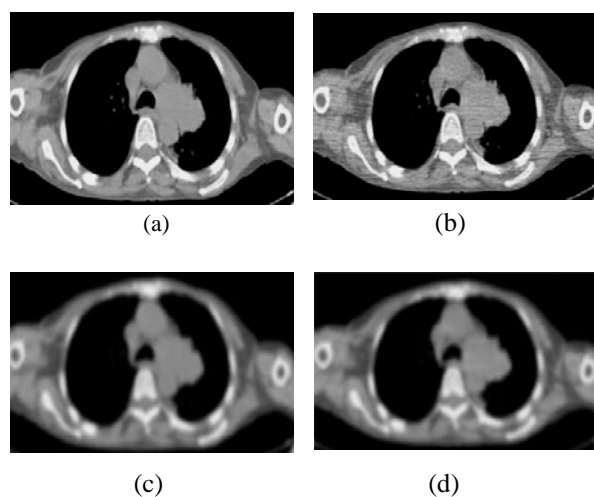

(a)   (b)

(c)   (d)

Figure 14. CT scans through the thorax acquired with 80 mA **(a)** and 10 mA **(b)** and corresponding attenuation map at 511 keV calculated using CTAC. Using CT at 80 mA **(c)**, and 10 mA **(d)**. Reprint with permission from ref. [58].

This is in contrast to relatively low effective doses of 0.15 mSv and 0.08 mSv for thoracic and whole-body transmission scans using positron emitting $^{68}Ga/^{68}Ge$ and single-photon emitting ^{137}Cs radionuclide sources, respectively [20]. With the introduction of PET/CT systems, several questions had to be answered, one of them is "to which limit can the CT tube current be reduced while still yielding adequate μmaps for attenuation correction of PET data?". Kamel *et al.* [58] investigated the effect of varying tube current and showed that a low-current CT is sufficient for CTAC using comparative quantitative analysis of reconstructed clinical PET images. Ay and Zaidi concluded that the attenuation map derivation is independent of tube current due to the fact the statistical fluctuation of CT numbers in the low current CT images removes during the down-sampling and smoothing process in CTAC method [96]. Likewise, a new pre-processing algorithm was proposed recently to use a single ultra-low dose CT scan for both attenuation map construction and lesion localization [97]. Figure 14 shows the CT scans at 80 and 10 mA, and corresponding attenuation map. The quality of the CT10 scan is clearly poorer than that of the CT80 scan. However, following degrading with a Gaussian filter and down-sampling, the calculate attenuation map from CT80 and CT10 scans look similar.

6. ^{18}F-FDG Imaging Protocol

The PET/CT scanner combines premier technology from two imaging modalities, making it possible to reveal both anatomical and functional information in a single procedure. Although combination of anatomical and functional imaging is an obvious

choice, the design of specific clinical protocols and flexible workflow utilities is still an active research arena and open to debate [34, 56, 98-103]. Figure 4 shows a standard PET/CT scanning protocol in currently available dual-modality systems. The standard ^{18}F-FDG imaging protocol is divided in seven different steps: (i) The patient is prepared form imaging which commonly include administration of both oral and IV contrast agents [42] and with typically 10 to 15 mCi ^{18}F-FDG in adults, that should be questioned independently for allergies to iodine-based CT contrast agents if these are to be administered intravenously during the course of a PET/CT study [34]. Proper patient preparation for PET studies has been described in detail, for example by Hamblen and Lowe [104]. (ii) The patient then is asked to remove all metal objects that may induce the streak artifact during the CT imaging; thereafter the patient is positioned on the patent table of the hybrid PET/CT scanner. (iii) The patient then undergoes a "topogram" or "scout" scan to identify the axial extend of CT imaging. (iv) The patient undergoes a helical CT acquisition with proper scan pitch and exposure settings in order to minimize the patient dose [60, 61]. (v) The patient then moves to the PET module of the PET/CT scanner and undergoes the emission scan. (vi) The CT and PET data are reconstructed and registered [105, 106], with the CT data also used for attenuation correction of PET data [107]. (vii) The images are reviewed quantitatively [108-110] and qualitatively [101] by a physician, who can view the CT, PET and hybrid images, followed by preparation of the associated clinical report. Qualitative visual assessment remains the principal method followed in the interpretation of routine clinical PET studies. However, visual interpretation intrinsically bears many important

weaknesses including the need to define a threshold for judgment of the existing and degree of radiotracer concentration [101]. Despite of the simplicity of visual interpretation it has limited application in research studies where more emphasize is put on quantitative analysis in order to allow more objective and reliable assessment [111]. The standard uptake value (SUV) is the most widely used quantitative uptake index in clinical PET studies. This parameter is define as the tissue concentration of tracer within a lesion divided by tissue density, as measured by PET, divided by the injected dose normalized to patient weight multiplied by a decay factor [112]. Since the weight is not always a good measure of initial tracer distribution volume, several investigators suggested variation on the SUV to account for this effect practically for obese patients. This include SUV using lean-body mass [113] or body surface area [114] in place of patient weight.

Generally two approaches can be distinguished for PET/CT protocols (Table 1). In the first scenario a high quality diagnostic CT is not needed, due to the fact the patient had previously undergone a complete CT examination. The low dose CT examination, as part of the PET/CT, is used only for generation of attenuation map for CTAC and also for anatomic labeling of PET findings. In the second scenario, a high quality diagnostic CT is clinically indicated. Typically, the CT, as part of the PET/CT, is acquired using oral or intravenous contrast agents to maximize the diagnostic information on anatomy and tumor vascularization. In addition, the CT is used for CTAC and anatomic labeling, or referencing of the PET results [34].

Regarding to the patient positioning, Beyer *et al.* [34] reported two main advises based on their experience on more than 3500 PET/CT studies: (i)

most patients should be scanned with arms raised and supported above the head. To facilitate comfortable positioning of the arms, several low-attenuation CT positioning devices are available. By raising the arms for the duration of the whole-body scan and leaving them outside the measured CT field of view, scatter artifacts in the body are much reduced and counting statistics of the corresponding emission scan are increased. Conversely, for head-and-neck investigations, the area is scanned with arms down. (ii) Independent of the coaxial imaging range, all patients should be supported with a proper knee rest for the duration of the combined scan. When using foam pallets or vacuum bags, no artifacts are typically introduced into the CT transmission scan. Table 2 summarizes some acquisition parameters in standard protocols.

7. Current Status and New Horizon in Hybrid Imaging

From advances in x-ray film and cassettes to the introduction of computers and digital images, diagnostic imaging has never stopped reinventing its technology to improve patient care. Today, diagnostic imaging is one of the cusps of explosive growth in an arena known as dual-modality imaging. This technology melds two independent imaging modalities (PET and CT), typically a procedure that demonstrates an organ's function and metabolism with one that depicts the organ's anatomy, to produce a diagnostically and clinically superior study. Until recently, clinicians had to obtain physiological and anatomical information on separate machines and use special registration software to digitally superimpose the two images. Today, new PET/CT dual-modality equipments are capable of performing both types of examinations simultaneously, automatically merging the data to form a composite image. By uniting metabolic function with anatomic form, dual-modality imaging depicts the human body with a level of precision never achieved before. In addition, the use of CT images for CT-based attenuation correction in dual-modality systems allows to decrease the overall scanning time and to create a noise free attenuation map [115]. However, still there are many technical issues that need to be solves through research [116]. Despite much worthwhile research performed during the last few years, artefacts induced by respiratory motion remain among the most difficult problems to solve [73].

Table 1: Objectives and requirements of clinical PET/CT imaging. Reprint with permission from ref. [34].

Scenario	Clinical approach	Focus group	Demands on CT	Demands on PET
CT for simple anatomic orientation	PET/CT replaces PET CT for fast attenuation correction and general anatomic orientation Mostly whole-body scans	Nuclear medicine	Low	High
CT for state-of-the-art diagnostic information	PET/CT replaces CT, or CT and PET State-of-the art diagnostic CT with contrast agents and standard exposure levels to maximize information on anatomy and tumor vascularization CT for fast attenuation correction Whole-body scans and dedicated protocols	Cross-modality, nuclear medicine, radiology, oncologist	High	High

Table 2. Diagnostic PET/CT acquisition parameters for whole-body and combined head/neck–torso protocol. Reprint with permission from ref. [34].

Protocol	Standard whole-body	Neck–Torso	
Imaging range	Whole-body	Torso	Neck
Topogram	1024 mm	756 mm	256 mm
CT contrast	140 mL: 90 mL at 3 mL/s, 50 mL at 1.5 mL/s	90 mL: 60 mL at 3 mL/s, 30 mL at 1.5 mL/s	60 mL: 60 mL at 3 mL/s
CT scan	Single-spiral 130 kVp, 110 mAs 0.8-s rotation time 5-mm slice width 8-mm table feed	Single-spiral 130 kVp, 100 mAs 0.8-s rotation time 5-mm slice width 8-mm table feed	Single-spiral 130 kVp, 160 mAs 0.8-s rotation time 3-mm slice width 5-mm table feed
Emission scan	3.5 min per bed 2 iterations and 8 subsets on 128 matrix with 5-mm Gaussian	3 min per bed 2 iterations and 8 subsets on 128 matrix with 5-mm Gaussian	4 iterations and 8 subsets on 256 matrix with 3-mm Gaussian, zoom 2
CT postprocessing	Lung window	Lung window	Zoomed head

Another limitation of current PET/CT technology is that sequential rather than simultaneous data acquisition is performed [117]. In addition the optimization of detector material, data acquisition electronics, geometrical design of detection system and image reconstruction algorithms are the active research area in the filed of hybrid imaging [8]. Over the years, there have been some moments at which the scientists might have felt that PET technology had reached its full potential and perhaps the major innovations were behind, but always some innovation change this idea [118]. In present and near future PET/CT is improving through implementation and optimization of respiratory gating algorithms, improving the count rates, more precise registration and the reintroduction of time of flight (TOF).

With a growing focus on cardiology applications, GE Healthcare strives to enhance image quality through dynamic, gated PET and volumetric CT (64 slice). The company introduced at the end of 2005 the Discovery VCT, a system that aims to convey a clearer view of the heart. The system combines PET's dynamic and gating data, acquiring a comprehensive view of the heart and coronary arteries with submillimeter resolution in five seconds, with volumetric CT used to visualize the anatomy of the heart's blood vessels. The VCT also features VUEPoint reconstruction [119], offering fully iterative reconstruction technology in 2-D and 3-D acquisition modes (Fig. 15).
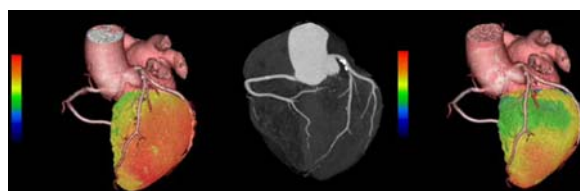

Figure 15. Discovery VCT first clinical case. O15 PET perfusion/ CT angiography (CTA).O15 rest perfusion (left), CTA (middle) and O15 stress perfusion (right). Courtesy Turku PET Center.

The angle that Siemens has carved out for improving PET/CT images is focusing on increased count rates. Siemens has adopted this approach by introducing TruePoint technology into its Biograph system. Designed for nuclear medicine applications where clinicians require extremely precise and

detailed images to pinpoint minute lesions and arteries, True Point reportedly adds 33 percent more axial volume coverage to its PET/CT scanner, extending the field of view and improving counts by more than 78 percent. More recently in the 2007 Society of Nuclear Medicine meeting, Siemens introduced their dedicated point spread function (PSF) reconstruction algorithm that called high definition PET (HD PET) [120]. HD PET incorporates millions of accurately measured point spread functions in the reconstruction algorithms. Using measured PSFs, HD PET effectively positions the LORs in their actual geometric location, which dramatically reduces blurring and distortion in the final image and offer the uniform resolution of almost 2 mm in entire FOV (Fig. 16).
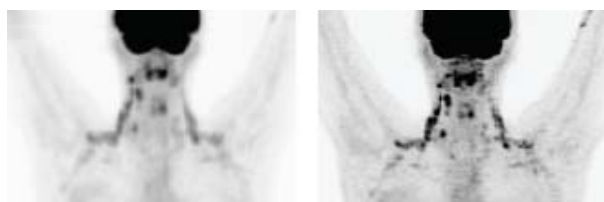

Figure 16. The difference between conventional PET (left) and HD PET (right) image quality. Data courtesy of the University of Erlangen.

Hitachi's SceptreP3 and GE's Discovery LS employ Dual Attenuation Correction (DAC) technology, which allows the combination of both CT and sealed source attenuation correction to effectively image patients with metal implants. In addition, the Non-Rigid Fusion algorithm provides precise registration by correcting for respiration differences between PET and CT acquisitions.

One technology used in PET imaging that has resurfaced in PET/CT systems is time-of-flight. The idea of TOF is not a new concept. TOF PET scanners

were developed in the 1980s and at that time were used chiefly in research [121-123]. In conventional PET, a valid event is formed when the two coincident 511keV annihilation photons are detected within some prespecified timing window, typically on the order of 5–12 ns for detectors based on scintillators. The two detectors in which interactions are measured determine a line along which the original annihilation site must lie. The location of the annihilation site along that line is unknown and must be recovered by image reconstruction. In TOF PET, the actual time difference in the arrival of the two annihilation photons at the detectors is recorded. The time difference increases the farther the annihilation site is from the point midway between the two detectors. Modern clinical PET scanners typically are capable of an isotropic spatial resolution in the 4 to 6 mm range. Therefore, if we wanted to use the TOF effect to pinpoint the annihilation site to about 5 mm and completely eliminate the need for image reconstruction, then the photon arrival times would need to be recorded with a precision of approximately 30 picoseconds. Detectors and electronics capable of such a timing resolution are not available; however, a timing resolution of a few hundred picoseconds is feasible. This can be used to constrain the reconstruction algorithm, because it localizes the annihilation site to within a few centimeters, and thus the reconstruction of that event can be weighted accordingly. With currently available electronic the TOF PET just improves the SNR without any improvement in spatial resolution (Fig. 17). Last year, Philips Medical Systems introduced the Gemini TF PET/CT, which provides what Philips calls TruFlight, its own version of TOF technology. The Gemini TF is a high-performance, fully 3-dimensional, time-of-flight PET scanner combined

with a Brilliance CT scanner (currently up to 64-slices). The PET scanner uses lutetiumyttrium oxyorthosilicate (LYSO) crystals that are placed in an Anger-logic detector, accomplishing a light spread in the detector that is uniform. The scanner was designed by Philips to be used as a high-performance conventional PET scanner in its own right, as well as a TOF scanner to provide improved timing resolution [124].

Not all manufacturers have bought into TOF because of certain limitations involving system requirements and respiratory gating, reason why GE Healthcare is not a proponent of the technology. Although TOF can improve image quality and reduce acquisition time, it requires a PET/CT system that has the highest sensitivity. GE contends that it already addresses the challenges of imaging bariatric patients with ViewPoint's reconstruction and 4-D imaging, which enhances image quality on patients of all sizes. Plus, unlike TOF, ViewPoint enables 4-D imaging for respiratory gating to essentially 'freeze' motion. According to one of its pioneers in the 1980s, a spokesperson at Siemens says TOF today is a

technology that may be worth adopting in the future because it can improve PET performance by enhancing count rates. However, Siemens' TruePoint technology is already doing this without TOF [125]. Whether PET/CT's performance is enhanced through respiratory gating for PET, better count rates, more precise registration or the reintroduction of TOF, each one of these enhancements contributes to faster image acquisition and better image quality with bariatric patients. The anatomically guide image reconstruction [29, 126] , new scatter correction techniques [18, 127], Spiral PET acquisition [7, 8] and implementation of partial volume correction algorithms in clinical area [21, 128, 129] are another potentials that might be enhanced the PET/CT imaging in near future. However, to have an idea about the specification of current PET?CT scanners some of the key parameters featured in the current range of PET/CT devices under market from different vendors are summarized in Table 3 [125].
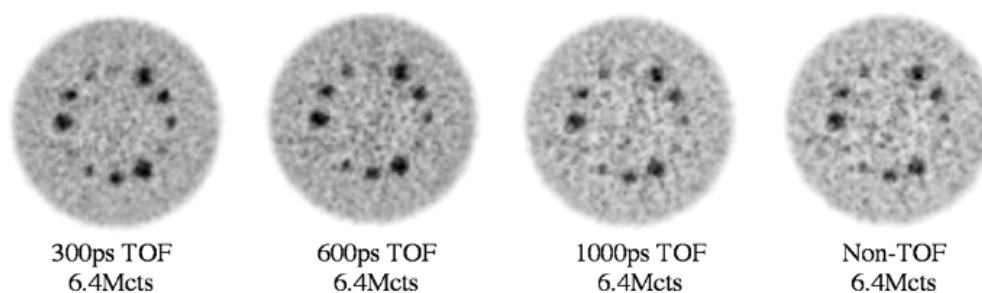

300ps TOF   600ps TOF   1000ps TOF   Non-TOF
6.4Mcts   6.4Mcts   6.4Mcts   6.4Mcts

Figure 17. Reconstructed images for the central slice in the 27-cm phantom. These images are for a fixed count statistics (6.4 Mcts). Moving left to right the images are: 300 ps TOF scanner, 600-ps TOF scanner, 1000-ps TOF scanner, and non-TOF scanner. Same scan times lead to improved image quality in a TOF scanner with better timing resolution. Reprint with permission from ref. [123].

Table 3. Some of the key parameters featured in the current range of PET/CT devices under market from different vendors (Data were colleted from the official web site of Imaging Technology News [125]).

Product Name	GEMINI GXL	GEMINI TF	Biograph TP	Discovery ST	Discovery STE	Discovery RX	Sceptre P3
Company	Philips	Philips	Siemens	GE	GE	GE	Hitachi
FDA-cleared	Yes	Yes	Yes	Yes	Yes	Yes	Yes
Acquisition modes	3D, 4D	3D, 4D	3D, 4D	2D, 3D, 4D	2D, 3D, 4D	2D, 3D, 4D	3D, 4D
Number of crystals	17,864	17,864	32448 (with TrueV)	10,080	13,440	15,120	4,224
Number of image planes	45 or 90	45 or 90	109 with TrueV	47	47	47	47
Crystal material	GSO	LYSO	LSO	BGO	BGO	LYSO	LSO
Ring diameter, cm	90	90	83	88.6	88.6	88.6	82.4
Axial FOV, cm	18	18	21.6 (with TrueV)	15.7	15.7	15.7	16.2
Crystal size, mm	4 x 6 x 30	4 x 4 x 22	4 x 4 x 20	6.2x 6.2x30	4.7x6.3x30	4.2 x6.3x30	6.45x6.45x25
Transverse resolution @ 1 cm, mm	5.3 (4.5 with LOR)	4.7 (4.3 with LOR)	4.2 (~2 with HD)	6.2 (2D) 6.2 (3D)	5.0 (2D) 5.0 (3D)	4.8 (2D) 4.8 (3D)	6.3
Transverse resolution@10 cm, mm	6.0	5.1	4.8 (~2 with HD)	6.8 (2D) 6.7 (3D)	5.7 (2D) 5.6 (3D)	5.3 (2D) 5.2 (3D)	6.8
System sensitivity - 3D (NEMA 2001)	8.0 cps/kBq	7.2 cps/kBq	7.9 cps/kBq (with TrueV)	9.3 cps/kBq	8.5 cps/kBq	8.0 cps/kBq	Unknown
System sensitivity - 2D (NEMA 2001)	NA	NA	NA	2.0 cps/kBq	2.0 cps/kBq	1.7 cps/kBq	NA
Scatter fraction-2D	NA	NA	NA	19%	19%	17%	NA
Scatter fraction-3D	37%	30%	36%	44%	35%	35%	36%
CT Module, Number of slice	6, 16	16, 64	6, 40, 64	4, 8, 16	8, 16, 64	16, 64	16
CT detector material	Solid-State GOS	Solid-State GOS	UltraFast Ceramic	Patented Ceramic	Patented Ceramic	Patented Ceramic	Ceramic

Most current commercial whole body PET/CT scanners employ conventional detector blocks consisting of several stacked rings of inorganic scintillating crystals radially oriented and readout on the backside by standard photomultiplier tubes (PMTs) or multi-anode PMTs. Another possible potential for enhancement of PET/CT's performance seems to be new geometrical concept for detection system. There are several new concepts including HPD PET [22], Pannel-base PET [8], large axial FOV PET [118] which are under development and might be commercially available in near future.

In principle all advantages of a PET/CT scanner could be replicated by PET/MRI; however, there are several major problems to combine PET and MRI technology in an integrated system. One obvious problem is that the radiation of interest, photons for PET and radiofrequency in MRI, come from opposite ends of the electromagnetic spectrum and there is no single detection system that can be used for both modalities. Besides putting the two machines in one cover, similar to the current PET/CT scanners design is problematic because of the incompatibility of currently used technologies in PET and MRI [8]. Historically, research on another multimodality combination, PET/MRI, started at roughly the same time as PET/CT, in the mid-1990s [130]. The immediate questions that come to mind regarding

PET/MRI are whether it is technically possible and what it will be used for. The earliest motivation for combined PET/MRI was the fact that strong magnetic fields can reduce the positron range effect [131]. Although one can debate how PET/MRI might ultimately be used, there is no doubting the technologic breakthroughs over the past 2 years that are now clearly demonstrating that simultaneous PET/MRI is possible. The earliest attempts at PET/MRI used optical fiber technology to pipe light from scintillators in the bore of a magnet to photomultiplier tubes, with good magnetic field immunity, in the fringe field outside the bore of the magnet [132-134]. PET/MR has four main additional features in comparison with PET/CT. First, for small animal studies, simultaneous scanning reduces time under anesthesia and enables scanning under identical physiological conditions. Second, high-field MRI generates high resolution anatomical and structural images offering better soft-tissue contrast resolution and a large variety of tissue contrasts compared to CT, and allows for functional MRI, thus enabling temporal correlation of blood flow with metabolism or receptor expression in brain studies and, more importantly, is capable of assessing flow, diffusion, perfusion, and cardiac motion in one single examination. Third, MRI can be combined with MRS to measure spatially matched regional biochemical content and to assess metabolic status or the presence of neoplasia and other diseases in specific tissue regions. Finally, MRI does not use any ionizing radiation and therefore can be used without restrictions in serial studies, for pediatric cases, and in many other situations where radiation exposure is a concern [135]. *"There is no doubt that in order to assess the need for PET/MR in a clinical setting, such a hybrid modality should be made available at least*

in large research centers. Results from studies conducted on these systems will then provide the necessary data to justify their routine clinical use and eventually convince the medical community about the merits and cost effectiveness of PET/MR. Until that happens, I believe that PET/CT will continue to be the modality of choice in whole body oncological imaging." PD. Dr. Habib Zaidi said in the month's Point/Counterpoint published in Journal of Medical Physics [135]. Considering the technology improvement in recent years the scientists expected to build the whole-body PET/MRI scanners in far future (5-10 years from now). Figure 18 shows the concept of whole-body PET/MRI scanner with large axial FOV PET [118].
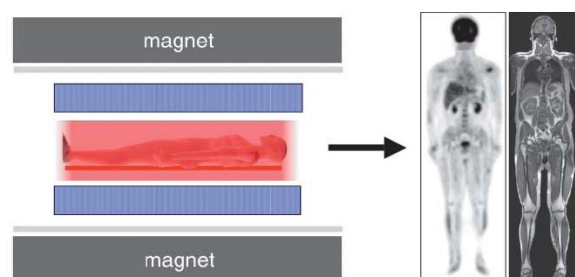

Figure 18. Concept of whole-body PET/MRI scanner, and images that such a system might produce (PET image courtesy of Siemens Medical Solutions; whole-body T1-weighted MR image courtesy of Dr. Heinz-Peter Schlemmer, University of Tubingen).Reprint with permission from ref. [118].

The obvious objection to such a system is one of expense in a financially restricted health care setting. To realize such a system in anything other than an elite medical research environment would require significant reductions in cost. But putting cost aside, technically, it is likely that the PET component of such a system could be built even with current technology, and as outlined here, the combination of PET and MRI is looking increasingly feasible. There

are certainly technologic challenges that would need to be addressed to fully realize the kinds of gains in PET that have been suggested. These challenges include the need to control the contribution of scattered coincidences (detectors with excellent energy resolution and perhaps some limited axial collimation) and random coincidences in a scanner that encompasses the whole body, the need for high-speed coincidence electronics to keep up with high data rates, and the need for fast and accurate iterative reconstruction algorithms to provide high-quality images in a reasonable time. But all of these challenges seem within our grasp [118].

8. Summary

PET/CT is the major tool for anato-metabolic imaging and now is performed routinely using ^{18}F-FDG to answer important questions including those in cardiology, neurology, psychiatry and oncology. The latter application contributed largely to the wide acceptance of this modality and its use in clinical diagnosis, staging, and assessment of tumor response to treatment. The use of CT images for CT-based attenuation correction in PET/CT allows to decrease the overall scanning time and to create a noise-free attenuation map in addition to improvement of lesion localization. Although the hybrid imaging is an obvious choice, the way to perform the right imaging is still an open issue considering the potential artifacts and errors in CTAC. In addition the tracers or combination of traces to be used, how the imaging should be done in presence of contrast agent, what is the optimum acquisition and processing protocol, what is the optimum quantitative analysis algorithm, are all still unanswered questions and need more research and development. Whether PET/MRI will succeed to replace PET/CT as the hybrid imaging platform of choice in future is still a debatable question that will retain the attention of active researchers in the filed during the next decade. Future advances in hybrid imaging instrumentation may come from unforeseen sources that are unknown yet, but they will come.

References

[1] Van den Elsen PA, Pol ED, and Viergever MA. Medical image matching- A review with classification. IEEE Trans. Eng. Med. Biol. 1993; 12: 26-39.

[2] Ay MR. Monte Carlo and experimental assessment of CT-based attenuation correction in PET. PhD. Thesis, 2005, Department of Radiology, Geneva: University of Geneva.

[3] Hasegawa BH, Stebler B, Rutt BK, Martinez A, Gingold EL, Barker CS, et al. A prototype high-purity germanium detector system with fast photon-counting circuitry for medical imaging. Med. Phys. 1991; 18: 900-909.

[4] Lang TF, Hasegawa BH, Liew SC, Brown JK, Blankespoor SC, Reilly SM, et al. Description of a prototype emission-transmission computed tomography imaging system. J Nucl Med. 1992; 33: 1881-1887.

[5] Hasegawa BH, Lang TF, Brown JK, Reilly SM, Blankespoor SC, Liew SC, et al. Object-specific attenuation correction of SPECT with correlated dual-energy x-ray CT. IEEE Trans. Nucl. Sci. 1993; 40: 1242-1252.

[6] Hasegawa BH and Zaidi H.Dual-modality imaging: more than the some of its components. in Quantitative analysis in nuclear medicine imaging, Zaidi H, Ed. New York: Springer, 2005; 35-81.

[7] Beyer T, Townsend DW, Brun T, Kinahan PE, Charron M, Roddy R, et al. A combined PET/CT scanner for clinical oncology. J Nucl Med. 2000; 41: 1369-1379.

[8] Townsend DW, Carney JPJ, Yap JT, and Hall NC. PET/CT today and tomorrow. J Nucl Med. 2004; 45: 4S-14S.

[9] Townsend DW, Beyer T, and Blodgett TM. PET/CT scanners: a hardware approach to image fusion. Semin Nucl Med. 2003; 33: 193-204.

[10] Osman MM, Cohade C, Nakamoto Y, Marshall LT, Leal JP, and Wahl RL. Clinically significant inaccurate localization of lesions with PET/CT: frequency in 300 patients. J Nucl Med. 2003; 44: 240-243.

[11] Kinahan PE, Fessler JA, Alessio AM, and Lewellen TK. Quantitative attenuation correction for PET/CT using iterative reconstruction of low-dose dual-energy CT. in *Proc.* IEEE Nuclear Science Symposium and Medical Imaging Conference., Oct. 19-22, Rome, Italy, 2004; 3285-3289.

[12] Beyer T, Tellmann L, Nickel I, and Pietrzyk U. On the use of positioning aids to reduce misregistration in the head and neck in whole-body PET/CT studies. J Nucl Med. 2005; 46: 596-602.

[13] Czernin J and Schelbert H. PET/CT imaging: facts, opinions, hopes, and questions. J Nucl Med. 2004; 45: 1S-3S.

[14] Vogel WV, Oyen WJ, Barentsz JO, Kaanders JH, and Corstens FH. PET/CT: panacea, redundancy, or something in between? J Nucl Med. 2004; 45 Suppl 1: 15S-24S.

[15] Hany TF, Steinert HC, Goerres GW, Buck A, and von Schulthess GK. PET diagnostic accuracy: improvement with in-line PET-CT system-initial results. Radiology. 2002; 225: 575-581.

[16] Kak AC and Slaney M. Principles of Computerized Tomographic Imaging. Electronic Copy ed., 1999. New York: IEEE PRESS.

[17] Turkington TG. Introduction to PET instrumentation. J. Nuc. Med. Technol. 2001; 29: 1-8.

[18] Zaidi H. Scatter modelling and correction strategies in fully 3D PET. Nucl Med Commun. 2001; 22: 1181-1184.

[19] Osman MM, Cohade C, Nakamoto Y, and Wahl RL. Respiratory motion artifacts on PET emission images obtained using CT attenuation correction on PET-CT. Eur J Nucl Med Mol Imaging. 2003; 30: 603-606.

[20] Zaidi H and Hasegawa BH. Determination of the attenuation map in emission tomography. J Nucl Med. 2003; 44: 291-315.

[21] Rousset OG, Ma Y, and Evans AC. Correction for partial volume effects in PET: principle and validation. J Nucl Med. 1998; 39: 904-911.

[22] Braem A, Llatas MC, Chesi E, Correia JG, Garibaldi F, Joram C, et al. Feasibility of a novel design of high resolution parallax-free compton enhanced PET scanner dedicated to brain research. Phys. Med. Biol. 2004; 49: 2547-2562.

[23] Sanchez-Crespo A, Andreo A, and Larsson SM. Positron flight in human tissues and its influence on PET image spatial resolution. Eur. J. Nucl. Med. 2003; 31: 44-51.

[24] Lonneux M, Borbath I, Bol A, Coppens A, Sibomana M, Bausart R, et al. Attenuation correction in whole-body FDG oncological studies: the role of statistical reconstruction. Eur J Nucl Med. 1999; 26: 591-598.

[25] Bailey DL. Transmission scanning in emission tomography. Eur J Nucl Med. 1998; 25: 774-787.

[26] Zaidi H, Montandon M-L, and Slosman DO. Magnetic resonance imaging-guided attenuation and scatter corrections in three-dimensional brain positron emission tomography. Med Phys. 2003; 30: 937-948.

[27] Zaidi H and Hasegawa B. Determination of the attenuation map in emission tomography. J. Nucl. Med. 2003; 44: 291-315.

[28] Kinahan PE, Hasegawa BH, and Beyer T. X-ray-based attenuation correction for positron emission tomography/computed tomography scanners. Semin Nucl Med. 2003; 33: 166-179.

[29] Comtat C, Kinahan PE, Fessler JA, Beyer T, Townsend DW, Defrise M, et al. Clinically feasible reconstruction of 3D whole-body PET/CT data using blurred anatomical labels. Phys Med Biol. 2002; 47: 1-20.

[30] Beyer T, Kinaham PE, Townsend DW, and Sashin D. The use of X-ray CT for attenuation correction of PET data. in *Proc.* IEEE Nuclear

Science Symposium and Medical Imaging Conference., Rome, Italy, 1995; 1573 - 1577.

[31] Kinahan PE, Townsend DW, Beyer T, and Sashin D. Attenuation correction for a combined 3D PET/CT scanner. Med Phys. 1998; 25: 2046-2053.

[32] Bai C, Shao L, Da Silva AJ, and Zhao Z. A generalized model for the conversion from CT numbers to linear attenuation coefficients. IEEE Trans Nucl Sci. 2003; 50: 1510-1515.

[33] Guy MJ, Castellano-Smith IA, Flower MA, Flux GD, Ott RJ, and Visvikis D. DETECT-dual energy transmission estimation CT-for improved attenuation correction in SPECT and PET. IEEE Trans Nucl Sci. 1998; 45: 1261 - 1267.

[34] Beyer T, Antoch G, Muller SP, Egelhof T, Freudenberg LS, Debatin JF, et al. Acquisition protocol considerations for combined PET/CT Imaging. J Nucl Med. 2004; 45: 25s-35s.

[35] Kinahan PE, Hasegawa B, and Beyer T. X-ray-based attenuation correction for positron emission tomography/computed tomography scanners. Semin. Nucl. Med. 2003; 34: 166-179.

[36] DiFilippo FP and Brunken RC. Do implanted pacemaker leads and ICD leads cause metal-related artifact in cardiac PET/CT? J Nucl Med. 2005; 46: 436-443.

[37] Goerres GW, Hany TF, Kamel E, von Schulthess GK, and Buck A. Head and neck imaging with PET and PET/CT: artifacts from dental metallic implants. Eur J Nucl Med Mol Imaging. 2002; 29: 367-370.

[38] Goerres GW, Ziegler SI, Burger C, Berthold T, Von Schulthess GK, and Buck A. Artifacts at PET and PET/CT caused by metallic hip prosthetic material. Radiology. 2003; 226: 577-584.

[39] Heiba SI, Luo J, Sadek S, Macalental E, Cacavio A, Rosen G, et al. Attenuation-correction induced artifact in F-18 FDG PET imaging following total knee replacement. Clin Positron Imaging. 2000; 3: 237-239.

[40] Kamel EM, Burger C, Buck A, von Schulthess GK, and Goerres GW. Impact of metallic dental implants on CT-based attenuation correction in a combined PET/CT scanner. Eur Radiol. 2003; 13: 724-728.

[41] Antoch G, Freudenberg LS, Beyer T, Bockisch A, and Debatin JF. To enhance or not to enhance? 18F-FDG and CT contrast agents in dual-modality 18F-FDG PET/CT. J Nucl Med. 2004; 45 Suppl 1: 56S-65S.

[42] Antoch G, Freudenberg LS, Stattaus J, Jentzen W, Mueller SP, Debatin JF, et al. Whole-body

[43] positron emission tomography-CT: optimized CT using oral and IV contrast materials. AJR Am J Roentgenol. 2002; 179: 1555-1560.

[43] Ay MR and Zaidi H. Assessment of errors caused by x-ray scatter and use of contrast medium when using CT-based attenuation correction in PET. Eur J Nucl Med Mol Imaging. 2006; 33: 1301-1313.

[44] Ay MR and Zaidi H. Simulation-based assessment of the impact of contrast medium on CT-based attenuation correction in PET. in Proceedings of IEEE Nuclear Science Symposium & Medical Imaging Conference, San Diego, USA, 2006; 3326-3330.

[45] Dizendorf E, Hany TF, Buck A, von Schulthess GK, and Burger C. Cause and magnitude of the error induced by oral CT contrast agent in CT-based attenuation correction of PET emission studies. J Nucl Med. 2003; 44: 732-738.

[46] Dizendorf EV, Treyer V, Von Schulthess GK, and Hany TF. Application of oral contrast media in coregistered positron emission tomography-CT. AJR Am J Roentgenol. 2002; 179: 477-481.

[47] Nakamoto Y, Chin BB, Kraitchman DL, Lawler LP, Marshall LT, and Wahl RL. Effects of nonionic intravenous contrast agents at PET/CT imaging: phantom and canine studies. Radiology. 2003; 227: 817-824.

[48] Nehmeh SA, Erdi YE, Kalaigian H, Kolbert KS, Pan T, Yeung H, et al. Correction for oral contrast artifacts in CT attenuation-corrected PET images obtained by combined PET/CT. J Nucl Med. 2003; 44: 1940-1944.

[49] Beyer T, Rosenbaum S, Veit P, Stattaus J, Muller SP, Difilippo FP, et al. Respiration artifacts in whole-body (18)F-FDG PET/CT studies with combined PET/CT tomographs employing spiral CT technology with 1 to 16 detector rows. Eur J Nucl Med Mol Imaging. 2005; 32: 1429-1439.

[50] Erdi YE, Nehmeh SA, Pan T, Pevsner A, Rosenzweig KE, Mageras G, et al. The CT motion quantitation of lung lesions and its impact on PET-measured SUVs. J Nucl Med. 2004; 45: 1287-1292.

[51] Goerres GW, Kamel E, Seifert B, Burger C, Buck A, Hany TF, et al. Accuracy of image coregistration of pulmonary lesions in patients with non-small cell lung cancer using an integrated PET/CT system. J Nucl Med. 2002; 43: 1469-1475.

[52] Goerres GW, Schmid DT, and Eyrich GK. Do hardware artifacts influence the performance of head and neck PET scans in patients with oral

cavity squamous cell cancer? Dentomaxillofac Radiol. 2003; 32: 365-371.

[53] Nehmeh SA, Erdi YE, Ling CC, Rosenzweig KE, Squire OD, Braban LE, et al. Effect of respiratory gating on reducing lung motion artifacts in PET imaging of lung cancer. Med Phys. 2002; 29: 366-371.

[54] Nehmeh SA, Erdi YE, Meirelles GS, Squire O, Larson SM, Humm JL, et al. Deep-inspiration breath-hold PET/CT of the thorax. J Nucl Med. 2007; 48: 22-26.

[55] Nehmeh SA, Erdi YE, Pan T, Pevsner A, Rosenzweig KE, Yorke E, et al. Four-dimensional (4D) PET/CT imaging of the thorax. Med Phys. 2004; 31: 3179-3186.

[56] Bockisch A, Beyer T, Antoch G, Freudenberg LS, Kuhl H, Debatin JF, et al. Positron emission tomography / computed tomography-Imaging protocols, artifacts, and pitfalls. Mol. Imag. Biol. 2004; 6: 188-199.

[57] Ay MR and Zaidi H. Computed Tomography-based attenuation correction in neurological positron emission tomography: evaluation of the effect of x-ray tube voltage on quantitative analysis. Nucl Med Commun. 2006; 27: 339-346.

[58] Kamel E, Hany TF, Burger C, Treyer V, Lonn AH, von Schulthess GK, et al. CT vs 68Ge attenuation correction in a combined PET/CT system: evaluation of the effect of lowering the CT tube current. Eur J Nucl Med Mol Imaging. 2002; 29: 346-350.

[59] Schaefer A, Seifert H, Donsch P, and Kirsch CM. Radiation exposure to patients caused by single-photon transmission measurement in PET. [German]. Nuklearmedizin. 2000; 39: 204-208.

[60] Wu T-H, Huang Y-H, Lee JS, Wang S-Y, Wang S-C, Su C-T, et al. Radiation exposure during transmission measurements: comparison between CT- and germanium-based techniques with a current PET scanner. Eur J Nucl Med Mol Imaging. 2004; 31: 38-43.

[61] Brix G, Lechel U, Glatting G, Ziegler SI, Munzing W, Muller SP, et al. Radiation exposure of patients undergoing whole-body dual-modality 18F-FDG PET/CT examinations. J Nucl Med. 2005; 46: 608-613.

[62] Krishnasetty V, Fischman AJ, Halpern EL, and Aquino SL. Comparison of alignment of computer-registered data sets: combined PET/CT versus independent PET and CT of the thorax. Radiology. 2005; 237: 635-639.

[63] Platten D. CT issues in PET/CT scanning. Medicines and Healthcare product Regulatory Agency (MHRA), London 2004.

[64] Qi J, Huesman R, and Reutter BW. Comparison of different CT-based attenuation correction schemes for PET with respiratory motion [abstract]. J Nucl Med. 2003; 44: 121.

[65] Goerres GW, Kamel E, Heidelberg TN, Schwitter MR, Burger C, and von Schulthess GK. PET-CT image co-registration in the thorax: influence of respiration. Eur J Nucl Med Mol Imaging. 2002; 29: 351-360.

[66] Goerres GW, Burger C, Schwitter MR, Heidelberg TN, Seifert B, and von Schulthess GK. PET/CT of the abdomen: optimizing the patient breathing pattern. Eur. Radiol. 2003; 13: 734-9.

[67] Nehmeh SA, Erdi YE, Pan T, Yorke E, Mageras GS, Rosenzweig KE, et al. Quantitation of respiratory motion during 4D-PET/CT acquisition. Med Phys. 2004; 31: 1333-1338.

[68] Nehmeh SA, Erdi YE, Rosenzweig KE, Schoder H, Larson SM, Squire OD, et al. Reduction of respiratory motion artifacts in PET imaging of lung cancer by respiratory correlated dynamic PET: methodology and comparison with respiratory gated PET. J Nucl Med. 2003; 44: 1644-1648.

[69] Pan T, Lee TY, Rietzel E, and Chen GT. 4D-CT imaging of a volume influenced by respiratory motion on multi-slice CT. Med Phys. 2004; 31: 333-340.

[70] Boucher L, Rodrigue S, Lecomte R, and Benard F. Respiratory gating for 3-dimensional PET of the thorax: feasibility and initial results. J Nucl Med. 2004; 45: 214-219.

[71] McClelland JR, Blackall JM, Tarte S, Chandler AC, Hughes S, Ahmad S, et al. A continuous 4D motion model from multiple respiratory cycles for use in lung radiotherapy. Med Phys. 2006; 33: 3348-3358.

[72] Nye JA, Esteves F, and Votaw JR. Minimizing artifacts resulting from respiratory and cardiac motion by optimization of the transmission scan in cardiac PET/CT. Med Phys. 2007; 34: 1901-1906.

[73] Visvikis D, Lamare F, Bruyant P, Boussion N, Turzo A, Bizais Y, et al. Respiratory motion in positron emission tomography for oncology applications: Problems and solutions. Nucl Instr Meth A. 2006; 569: 453-457.

[74] Beyer T, Antoch G, Blodgett T, Freudenberg LF, Akhurst T, and Mueller S. Dual-modality PET/CT imaging: the effect of respiratory motion on combined image quality in clinical

oncology. Eur J Nucl Med Mol Imaging. 2003; 30: 588-596.

[75] Pan T, Mawlawi O, Nehmeh SA, Erdi YE, Luo D, Liu HH, et al. Attenuation correction of PET images with respiration-averaged CT images in PET/CT. J Nucl Med. 2005; 46: 1481-1487.

[76] Alessio AM, Kinahan PE, Cheng PM, H. V, and Karp JS. PET/CT scanner instrumentation, challenges, and solutions. Radiol Clin North Am. 2004; 42: 1017-1032.

[77] Beyer T, Bockisch A, Kuhl H, and Martinez MJ. Whole-body 18F-FDG PET/CT in the presence of truncation artifacts. J Nucl Med. 2006; 47: 91-99.

[78] Mawlawi O, Erasmus JJ, Pan T, Cody DD, Campbell R, Lonn AH, et al. Truncation artifact on PET/CT: impact on measurements of activity concentration and assessment of a correction algorithm. AJR Am J Roentgenol. 2006; 186: 1458-1667.

[79] Sureshbabu W and Mawlawi O. PET/CT imaging artifacts. J Nucl Med Technol. 2005; 33: 156-161.

[80] Carney JP, Townsend DW, Kinahan PE, Beyer T, Kachelriess K, De Man B, et al. CT-based attenuation correction: the effect of imaging with the arms in the field-of-view. J. Nucl. Med. 2001; 42: 56P-57P.

[81] Joseph PM and Ruth C. A method for simultaneous correction of spectrum hardening artifact in CT images containing both bone and iodine. Med. Phys. 1997; 24: 100-108.

[82] Zaidi H and Ay MR. Impact of x-ray scatter when using CT-based attenuation correction in PET: A Monte Carlo investigation. in Proceedings of IEEE Nuclear Science Symposium & Medical Imaging Conference, San Diego, USA, 2006; 2161-2165.

[83] Hasegawa BH, Iwata K, Wong KH, Wu MC, Da Silva AJ, Tang HR, et al. Dual-modality imaging of function and physiology. Acad Radiol. 2002; 9: 1305-1321.

[84] Antoch G, Kuehl H, Kanja J, Lauenstein TC, Schneemann H, Hauth E, et al. Dual-modality PET/CT scanning with negative oral contrast agent to avoid artifacts: introduction and evaluation. Radiology. 2004; 230: 879-885.

[85] Antoch G, Saoudi N, Kuehl H, Dahmen G, Mueller SP, Beyer T, et al. Accuracy of whole-body dual-modality fluorine-18-2-fluoro-2-deoxy-D-glucose positron emission tomography and computed tomography (FDG-PET/CT) for tumor staging in solid tumors: comparison with CT and PET. J Clin Oncol. 2004; 22: 4357-4368.

[86] Groves AM, Kayani I, Dickson JC, Townsend C, Croasdale I, Syed R, et al. Oral contrast medium in PET/CT: should you or shouldn't you? Eur J Nucl Med Mol Imaging. 2005; 32: 1160-1166.

[87] Yau Y-Y, Chan W-S, Tam Y-M, Vernon P, Wong S, Coel M, et al. Application of intravenous contrast in PET/CT: does it really introduce significant attenuation correction error? J Nucl Med. 2005; 46: 283-291.

[88] Berthelsen AK, Holm S, Loft A, Klausen TL, Andersen F, and Hojgaard L. PET/CT with intravenous contrast can be used for PET attenuation correction in cancer patients. Eur J Nucl Med Mol Imaging. 2005; 32: 1167-1175.

[89] Tang HR, Brown JK, Da Silva AJ, Matthay KK, Price DC, Huberty JP, et al. Implementation of a combined X-ray CT-scintillation camera imaging system for localizing and measuring radionuclide uptake: experiments in phantoms and patients. IEEE Trans Nucl Sci. 1999; 46: 551-557.

[90] Buther F, Stegger L, Dawood M, Range F, Schafers M, Fischbach R, et al. Effective methods to correct contrast agent-induced errors in PET quantification in cardiac PET/CT. J Nucl Med. 2007; 48: 1060-1068.

[91] Bidgoli J, Ay M, Sarkar S, Ahmadian A, and Zaidi H. Correction of oral contrast artifacts in CT-based attenuation correction of PET images using an automated segmentation algorithm. in Proceedings of IEEE Nuclear Science Symposium & Medical Imaging Conference, Hawaii, USA, 2007; *in press*.

[92] Ay MR, Bidgoli JH, Sarkar S, and Ahmadian A. Automatic segmentation of oral contrast enhanced CT images for artifact free attenuation correction in PET/CT. in Annual Congress of the European Association of Nuclear Medicine Copenhagen, Denmark, 2007.

[93] Carney JP, Townsend DW, Rappoport V, and Bendriem B. Method for transforming CT images for attenuation correction in PET/CT imaging. Med Phys. 2006; 33: 976-983.

[94] Rappoport V, Carnry JPJ, and Townsend DW. CT tube-voltage dependent attenuation correction scheme for PET/CT scanners. in IEEE Nuclear Science Symposium and Medical Imaging Conference, Oct. 19-22, Rome, Italy, 2004; 3853-3857.

[95] Berger MJ and Hubbell JH. XCOM: Photon cross sections on a personal computer. National Bureau of Standards (US), Gaithersburg, MD NBSIR 87-3597, 1987.

[96] Ay MR and Zaidi H. Impact of x-ray tube settings and metallic leads on neurological PET imaging when using CT-based attenuation correction. Nucl Instr Meth A. 2006; 571: 411-417.

[97] Li J, Hsieh J, Colsher J, Stearns C, and Lonn AHR. Towards single ultra-low dose CT scan for both attenuation map creation and localization in PET-CT application. in *Proc. IEEE Nuclear Science Symposium and Medical Imaging Conference*, Oct. 19-22, Rome, Italy, 2004; 2396-2398.

[98] Brechtel K, Klein M, Vogel M, Mueller M, Aschoff P, Beyer T, et al. Optimized contrast-enhanced CT protocols for diagnostic whole-body 18F-FDG PET/CT: technical aspects of single-phase versus multiphase CT imaging. J Nucl Med. 2006; 47: 470-476.

[99] Wu TH, Chu TC, Huang YH, Chen LK, Mok SP, Lee JK, et al. A positron emission tomography/computed tomography (PET/CT) acquisition protocol for CT radiation dose optimization. Nucl Med Commun. 2005; 26: 323-330.

[100] Blodgett TM, McCook BM, and Federle MP. Positron emission tomography/computed tomography: protocol issues and options. Semin Nucl Med. 2006; 36: 157-168.

[101] Zaidi H. Optimization of whole-body PET/CT scanning protocols. Biomed Imaging Interv J. 2007; 3: *in press*.

[102] Pfannenberg AC, Aschoff P, Brechtel K, Muller M, Bares R, Paulsen F, et al. Low dose non-enhanced CT versus standard dose contrast-enhanced CT in combined PET/CT protocols for staging and therapy planning in non-small cell lung cancer. Eur J Nuc Med Mol Imaging. 2007; V34: 36-44.

[103] Gilman MD, Fischman AJ, Krishnasetty V, Halpern EF, and Aquino SL. Optimal CT breathing protocol for combined thoracic PET/CT. AJR Am J Roentgenol. 2006; 187: 1357-1360.

[104] Hamblen B and Lowe VJ. Clinical 18F-FDG oncology patient preparation techniques. J Nucl Med Technol. 2003; 31: 3-10.

[105] Landmann M and Glatting G. Quantitative image reconstruction in PET from emission data only using cluster analysis. Z Med Phys. 2003; 13: 269-274.

[106] Mesina CT, Boellaard R, Jongbloed G, van der Vaart AW, and Lammertsma AA. Experimental evaluation of iterative reconstruction versus filtered backprojection for 3D [15O]water PET activation studies using statistical parametric mapping analysis. Neuroimage. 2003; 1: 1170-1179.

[107] Visvikis D, Costa DC, Croasdale I, Lonn AHR, Bomanji J, Gacinovic S, et al. CT-based attenuation correction in the calculation of semi-quantitative indices of [18F]-FDG uptake in PET. Eur J Nucl Med. 2003; 30: 344-353.

[108] Eckelman W, Tatum J, Kurdziel K, and Croft Y. Quantitative analysis of tumor biochemistry using PET and SPECT. Nucl Med Biol. 2000; 27: 633-635.

[109] Bailey DL.Quantitative procedures in 3D PET. in The theory and practice of 3D PET., Bendriem B and Townsend DW, Eds. Dordrecht, The Netherlands: Kluwer Academic Publishers, 1998; 55-109.

[110] Montandon M-L and Zaidi H. Quantitative analysis of template-based attenuation compensation in 3D brain PET. Comput Med Imaging Graph. 2007; 31: 28-38.

[111] Acton PD, Zhuang H, and Alavi A. Quantification in PET. Radiol Clin North Am. 2004; 42: 1055-1062.

[112] Thie JA. Understanding the standardised uptake value, its method, and implications for usage. J Nucl Med. 2004; 45: 1431-1434.

[113] Zasadny KR and Wahl R. Standardized uptake values of normal tissues at PET with 2-[fluorine-18]-fluoro-2-deoxy-D-glucose: variations with body weight and a method for correction. Radiology. 1993; 189: 847-850.

[114] Kim CK and Gupta NC. Dependency of standardized uptake values of fluorine-18 fluorodeoxyglucose on body size: comparison of body surface area correction and lean body mass correction. Nucl Med Comm. 1996; 17: 890-894.

[115] Alavi A, Lakhani P, Mavi A, Kung JW, and Zhuang H. PET: a revolution in medical imaging. Radiol Clin North Am. 2004; 42: 983-1001.

[116] Zaidi H. The quest for the ideal anato-molecular imaging fusion tool. Biomed Imaging Interv J. 2006; 2: e47.

[117] Alavi A, Mavi A, Basu S, and Fischman A. Is PET-CT the only option? Eur J Nuc Med Mol Imaging. 2007; 34: 819-821.

[118] Cherry SR. The 2006 Henry N. Wagner Lecture: Of Mice and Men (and Positrons)—Advances in PET Imaging Technology. J Nucl Med. 2006; 47: 1735-1745.

[119] Vernon P. VUE Point:bringing accuracy to PET reconstruction. GE Healthcare, Waukesha, USA 2005.

[120]   Casey ME. Point spread function reconstruction in PET. Siemens Medical Solution, Knoxville, USA 2007.

[121]   Lewellen TK. Time-of-flight PET. Semin Nucl Med. 1998; 28: 268-275.

[122]   Moses WW. Time of flight in PET revisited. IEEE Trans Nucl Sci. 2003; 50: 1325-1330.

[123]   Surti S, Karp JS, Popescu LM, Daube-Witherspoon M, and Werner M. Investigation of Time-of-Flight benefit for fully 3-D PET. IEEE Trans Med Imaging. 2006; 25: 529-538.

[124]   Surti S, Kuhn A, Werner M, Perkins AE, Kolthammer J, and Karp JS. Performance of Philips Gemini TF PET/CT scanner with special consideration for its time-of-flight imaging capabilities. J Nucl Med. 2007; 48: 471-480.

[125]   Imaging Technology News. http://www.itnonline.net, 2007.

[126]   Delbeke D, Martin WH, Patton JA, and Sandler MP. Value of iterative reconstruction, attenuation correction, and image fusion in the interpretation of FDG PET images with an integrated dual-head coincidence camera and X-ray-based attenuation maps. Radiology. 2001; 218: 163-171.

[127]   Watson CC. New, faster, image-based scatter correction for 3D PET. IEEE Trans Nucl Sci. 2000; 47: 1587-1594.

[128]   Meltzer CC, Kinahan PE, Greer PJ, Nichols TE, Comtat C, Cantwell MN, et al. Comparative evaluation of MR-based partial-volume correction schemes for PET. J Nucl Med. 1999; 40: 2053-2065.

[129]   Pretorius PH, King MA, and Bruvant PP. Influence of mismatched CT anatomy on the accuracy of partial volume compensation in cardiac SPECT perfusion imaging. in Nuclear Science Symposium Conference Record, 2004 IEEE, 2004; 3213-3216.

[130]   Shao Y, Cherry SR, Farahani K, Meadors K, Siegel S, Silverman RW, et al. Simultaneous PET and MR imaging. Phys Med Biol. 1997; 10: 1965-1970.

[131]   Raylman RR, Hammer BE, and Christensen NL. Combined MRI-PET scanner: a Monte-Carlo evaluation of the improvements in PET resolution due to the effects of a static homogeneous magnetic field. IEEE Trans Nucl Sci. 1996; 43: 2406-2412.

[132]   Seemann MD. Whole-body PET/MRI: the future in oncological imaging. Technol Cancer Res Treat. 2005; 4: 577-582.

[133]   Pichler BJ, Judenhofer MS, Catana C, Walton JH, Kneilling M, Nutt RE, et al. Performance test of an LSO-APD detector in a 7-T MRI scanner for simultaneous PET/MRI. J Nucl Med. 2006; 47: 639-647.

[134]   Gaa J, Rummeny EJ, and Seemann MD. Whole-body imaging with PET/MRI. Eur J Med Res. 2004; 30: 309-312.

[135]   Zaidi H and Mawlawi O. Simultaneous PET/MR will replace PET/CT as the molecular multimodality imaging platform of choice. Med Phys. 2007; 34: 1525-1528.